Fast ion charge exchange spectroscopy adapted for tangential viewing geometry in LHD[a)]

T. Ito,[1] M. Osakabe,[1] K. Ida,[1] M. Yoshinuma,[1] M. Kobayashi,[1] M. Goto,[1] S. Murakami,[2] M. Isobe,[1] S. Kobayashi,[2] K. Toi,[1] K. Ogawa,[3] Y. Takeiri,[1] and S. Okamura[1]
[1]*National Institute for Fusion Science, Toki 509-5292, Japan*
[2]*Department of Nuclear Engineering, Kyoto University, Kyoto 606-8501, Japan*
[3]*Department of Energy Engineering and Science, Nagoya University, Nagoya 464-8601, Japan*

(Presented 17 May 2010; received 18 May 2010; accepted 24 September 2010; published online 28 October 2010)

A tangential Fast Ion Charge eXchange Spectroscopy is newly applied on a Large Helical Device (LHD) for co/countercirculating fast ions, which are produced by high energy tangential negative-ion based neutral beam injection. With this new observation geometry, both the tangential-neutral beam (NB) and a low-energy radial-NB based on positive ions can be utilized as probe beams of the measurement. We have successfully observed Doppler-shifted H-alpha lights due to the charge exchange process between the probing NB and circulating hydrogen ions of around 100 keV in LHD plasmas. © *2010 American Institute of Physics.* [doi:10.1063/1.3502331]

I. INTRODUCTION

In the fusion reactor, fast ions play important roles in sustaining plasmas by heating with fusion-born alpha particles and also in sustaining magnetic configurations by the current drive with fast ions being produced by tangentially injected neutral beam (NB).[1] Since behaviors of fast ions in magnetically confined plasmas can be affected by the ripples of magnetic fields and also by instabilities in plasmas, these efficiencies might degrade with these influences. Therefore, it is important to investigate the confinement properties of fast ions in magnetic fusion devices.

A new fast-ion diagnostic based on charge exchange spectroscopy called Fast Ion Charge eXchange Spectroscopy (FICXS) has been applied on Large Helical Device.[2] In this diagnostic, the Doppler-shifted Hα lights from fast neutrals are utilized as signals of fast ions, where these fast neutrals are produced by the charge exchange process between fast ions in plasmas and injected NBs. The diagnostic is similar to the fast ion deuterium alpha measurement[3,4] where the Doppler-shifted Dα lights are used. The advantages of these CXS based fast-ion diagnostic are the locality of the measurement on its line of sight (LOS) and the easiness for applying it to the spatial measurement.

The interactions between cogoing fast ions and Alfvén eigenmode (AE) are reported on Large Helical Device (LHD).[5] It is considered to be important to evaluate the spatial profile of a fast ion having their kinetic energies largely parallel to the magnetic field lines since the spatial profile of parallel fast-ion component is strongly related to the Alfvénic phenomena. Moreover, it is recently recognized that the transport of parallel fast ions might more seriously suffer from the influences of turbulences in plasmas than that of perpendicular fast ions. On LHD, we have newly installed FICXS diagnostic of tangential viewing geometry to investigate the confinement property of parallel fast ions. The major challenge of tangential FICXS (t-FICXS) diagnostic on LHD is the small reaction rate of charge exchange process for passing fast ions since these fast ions are produced by negative hydrogen-ion based high energy NBs of up to 190 keV. For example, the reaction rate for charge exchange process between hydrogen neutral and ion is maximized at around the ~40 keV and starts to decrease as the energy increases. The reaction rate decreases to about two orders in magnitude from its maximum value at the injection energy of the LHD-NBI.

This article is organized as follows. Section II explains the geometrical arrangement and instrument of FICXS diagnostic. Section III presents typical observation of fast ion charge exchange (FICX) spectrum in tangential viewing geometry. Section IV discusses the observable range of energy distribution of fast ion measured by the FICXS diagnostic. The conclusions are summarized in Sec. V.

II. EXPERIMENTAL SETUP

The geometrical arrangement of t-FICXS diagnostic on LHD is shown in Fig. 1. The LOSs are horizontally aligned and the radial distributions of Doppler-shifted H_α emitted from parallel fast ions can be measured with this arrangement. Two tangential NBIs (NBI 1 and NBI 2) are utilized as a main source of fast ions. The other tangential NBI (NBI 3) and a radial NBI (NBI 4) can be used for sources of active neutrals of the FICXS measurement. However, in this paper, we only show the measurement of passing particles with NBI 4, since NBI 3 also works as a source of fast ions and makes the measurement complicated. The measurement region locates in horizontally elongated poloidal cross section and covers from magnetic axis to the inboard edge of LHD plasmas. This corresponds to the major radius R ~ 2.8 m to

[a)]Contributed paper, published as part of the Proceedings of the 18th Topical Conference on High-Temperature Plasma Diagnostics, Wildwood, New Jersey, May 2010.

 © 2010 American Institute of Physics

Downloaded 19 Jun 2011 to 130.54.110.71. Redistribution subject to AIP license or copyright; see http://rsi.aip.org/about/rights_and_permissions

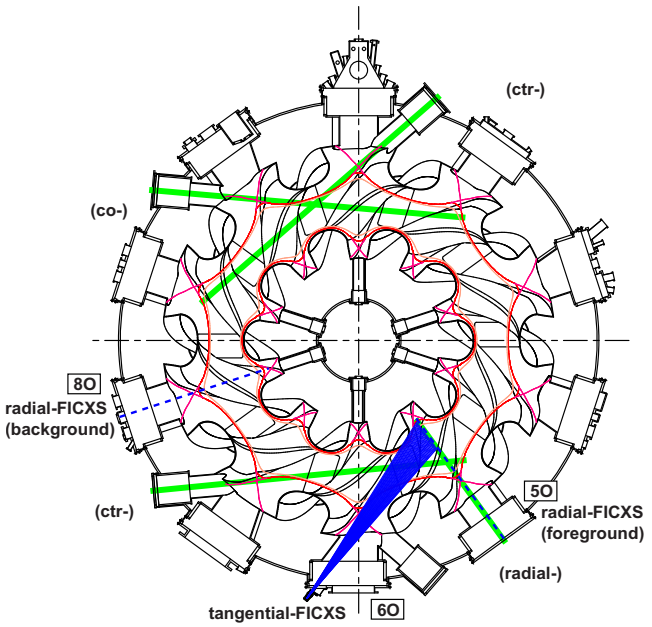

FIG. 1. (Color online) Midplane view of LHD showing the tangential sightlines of FICXS diagnostic and the traces of three tangential NBIs.

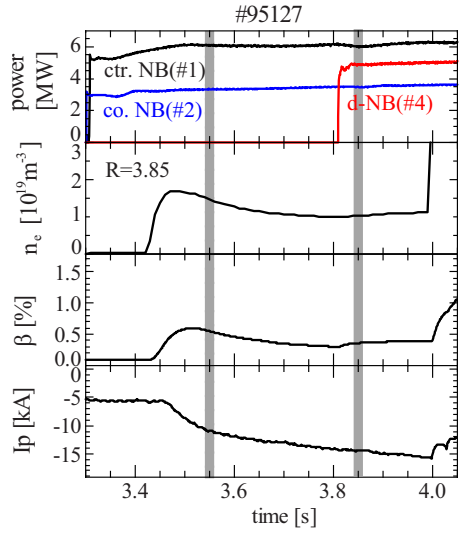

FIG. 2. (Color online) Waveform of typical discharge for observation of FICXS measurement.

~3.8 m. The background of the measurement is evaluated by the switching-off the NBI 4 because the background LOSs are not available in t-FICXS measurement.

The Doppler-shifted Hα lights are collected and are transferred by the bundled 41ch optical fibers (200 μm) to the single spectrometer (BUNKOKEIKI/HTP-400E). The spectrometer has a grating number of 2160/mm, focal length of 400 mm, and the F=2.8. Observation range of wavelength can be changed by controlling grating angle. No filter is placed in the optics because the wavelength range of the spectrometer is narrow enough to separate bulk Hα light from the CX observation domain. Finally, the collected lights are recorded by the charged-coupled device. The exposure time of the measurement is set to 150 ms, while the sampling interval is set to 300 ms.

III. TYPICAL OBSERVATION

The typical discharge waveforms for t-FICXS measurement are shown in Fig. 2. The measurement was performed by the switching on NBI 4 (39.5 keV) during the plasmas are sustained by NBI 1 (190.5 keV) and NBI 2 (164.3 keV). In this observation geometry, the FICX Hα light due to NBI 1 shift to the red side, while that due to NBI 2 shift to blue-side. Figure 3(a) shows the observed FICX spectra. In this case, the measured spectral range was set between 661 and 666 nm. This range is the redshift side of Hα light, thus the observed spectra is due to the fast ions produced by NBI 1. The red curves in Fig. 3(a) show the spectra at around t =3.85 s that correspond to the foreground measurement with NBI 4. On the other hand, the black curves in the figure are the spectra at t=3.55 s. These are the spectra without NBI 4 and correspond to the background measurement. The FICX spectra are obtained by subtracting the background spectra from the foreground and are shown by black curves in Fig. 3(b). The several impurity lines are observed both in the foreground and the background spectra, and their species have not been identified, yet. Fortunately, the most of the impurity lines were removed by the background subtraction except for the large residue from the strong impurity line around 663.6 nm, as shown in Fig. 3(b). This might be the charge exchange component of impurity lines. The bremsstrahlung radiation was also removed by the subtraction by the background bin because the electron density is almost stationary during the measurement.

In Fig. 3(b), the evaluated FICX-spectra using the result of computer simulation code is also shown. In the simulation, the fast-ion distribution function was derived from

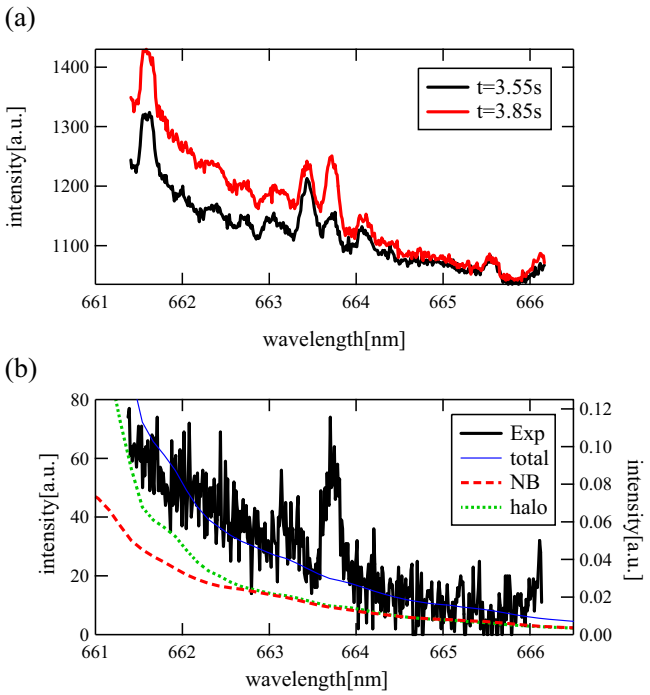

FIG. 3. (Color online) (a) Measured spectra when NBI 4 turned on (t=3.85 s) and turned off (t=3.55 s). (b) Solid curve shows the FICX component obtained by the subtraction from "signal" to "background." Dashed, dotted, and thin curves indicate the reconstructed spectra for the probe beam, the halo neutral, and their summation, respectively.

Downloaded 19 Jun 2011 to 130.54.110.71. Redistribution subject to AIP license or copyright; see http://rsi.aip.org/about/rights_and_permissions

GNET code,[6] which solves the drift kinetic equation in two-dimensional velocity space and in three-dimensional (3D) real space. The NB attenuation profile was calculated by NBATTEN-code.[2] The halo neutral, which was created by the charge exchange process between bulk ions and injected neutrals by NBI 4, the distribution was evaluated by using 3D neutral transport code (EIRENE-3D code[7]). In Fig. 3(b), the FICX-spectra with the charge exchange process between fast ions and NB are shown in red (NB-FICX component), while the spectra between fast ions and halo neutrals are shown in green (halo-FICX component). The blue curves indicate the sum of these two components. As shown in the figure, the observed FICX spectrum appears at the expected range in wavelength and its shape is similar to the summed spectra. This indicates the observation of the tangential FICX spectra is successful.

Both NB-FICX and halo-FICX components show similar spectral shape in the region where the wavelengths are greater than 663 nm. The halo component becomes slightly larger in the wavelengths less than 663 nm because the relative velocity between the halo neutrals and fast ions become more suitable for CX reaction than that between fast ions and NB particles.

IV. DISCUSSION

Since both NB-FICX and halo-FICX components contain the information of fast ions, the signal intensities that are integrated in certain wavelength ranges in the observed spectra represent the fast ions in certain energy ranges. Thus, the integrated signal can be used to evaluate the confinement properties of fast ions on LHD during its slowing down process.

In Fig. 4(a), the lines of sight for tangential FICXS measurement on LHD are shown. The observed spectra shown in Fig. 3(b) are obtained in the sight line of 37, which is indicated by a thick blue line. In the figure, the attenuated NB-profiles on the sight lines are also shown. As shown in the figure, the NB profile on LOS 37 is peaked at $\rho=0.15$. The full width at half maximum of the NB-profile on the LOS gives an ambiguity of 0.06 in ρ. Figure 4(b) shows evaluated velocity distributions of fast ions that contributes to the FICXS signals in region-A (661.5–663 nm) and region-B (664.2–665.8 nm) in Fig. 3(b). The signals in the region-A are shown by the yellow to red area at around $v_{\parallel}=-3\times10^{6}$ m/s. The energies of fast ions in the region are mainly between 30 and 50 keV. On the other hand, signals in range-B comes from the red area around $v_{\parallel}=-4\times10^{6}$ m/s, where the energies of fast ions in the region are mainly between 70 and 100 keV. As shown in Fig. 4(b), these two regions are well isolated to each other and well represent groups of fast ion corresponding to each energy ranges. It seems that the energy of 100 keV is the upper limit for hydrogenic ions in this observation geometry using the radial NBI. The use of tangential-NBI (NBI 3) might extend the observable energy range of the measurement since the relative velocity between the fast ions and probing beam becomes preferable.

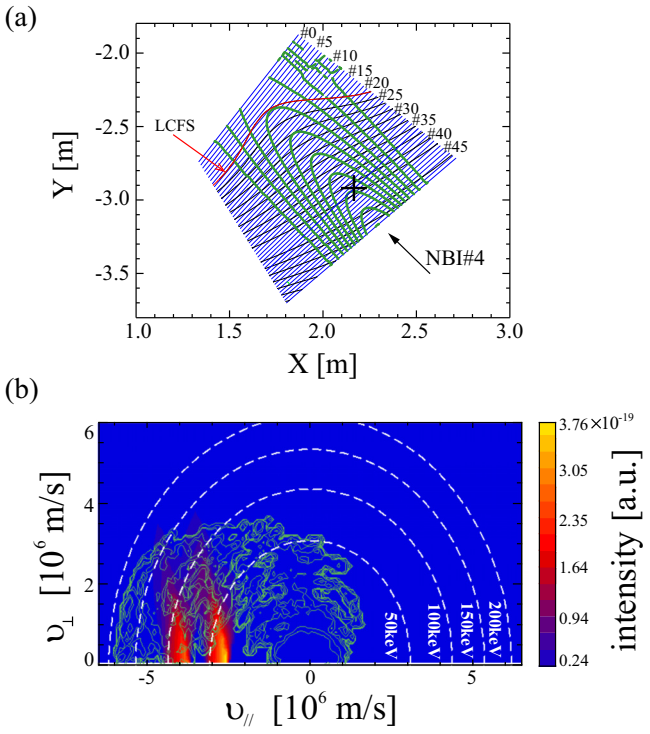

FIG. 4. (Color online) (a) A schematic drawing of the observation geometry for tangential FICXS measurement on LHD. The thin lines show the LOSs for tangential FICXS measurement, while bold solid curves indicate the profile of NB 4 on the LOSs. The black curves show flux surfaces of the plasma. (b) Velocity distributions of fast ions that contribute to the FICXS signals in certain wavelength ranges are shown. The distribution is obtained for the point indicated by horizontal cross in (a). A typical velocity distribution of fast ions is also shown by thin contours. The distribution for the region-A and region-B in Fig. 3(b) are also shown by the faded areas.

V. CONCLUSION

A tangential FICXS diagnostic was installed to investigate the confinement properties of parallel fast-ion components on LHD. In the current configuration, the hydrogenic ions of up to 100 keV, which has comparable velocity of deuterium ions of 200 keV, are successfully obtained by tangential FICXS measurement with radially injected NBs. By selecting the range in wavelength and integrating the spectra in the range, it was shown that the integrated signals well represent the fast ions in the corresponding energy ranges. Thus, the comparison between the integrated signals in different wavelength ranges will provide us a good knowledge of fast-ion confinement properties during its slowing down process on LHD.

ACKNOWLEDGMENTS

The support of the LHD experiment group is gratefully acknowledged. This work is supported by the LHD project budget Contract Nos. NIFS09ULBB512, NIFS09KLBB301, NIFS09ULBB510, and NIFS09KLBB301. This work also partly supported by the Grant-in-aid for Scientific Research from JSPS Grant Nos. 18340189, 21360457, and 22860076.

[1] A. Fasoli, C. Gormenzano, H. L. Berk, B. Breizman, S. Briguglio, D. S. Darrow, N. Gorelenkov, W. W. Heidbrink, A. Jaun, S. V. Konovalov, R. Nazikian, J.-M. Noterdaeme, S. Sharapov, K. Shinohara, D. Testa, K. Tobita, Y. Todo, G. Vlad, and F. Zonca, Nucl. Fusion **47**, S264 (2007).

Downloaded 19 Jun 2011 to 130.54.110.71. Redistribution subject to AIP license or copyright; see http://rsi.aip.org/about/rights_and_permissions

[2] M. Osakabe, S. Murakami, M. Yoshinuma, K. Ida, A. Whiteford, M. Goto, D. Kato, T. Kato, K. Nagaoka, T. Tokuzawa, Y. Takeiri, and O. Kaneko, Rev. Sci. Instrum. **79**, 10E519 (2008).
[3] W. W. Heidbrink, K. H. Burrell, Y. Luo, N. A. Pablant, and E. Ruskov, Plasma Phys. Controlled Fusion **46**, 1855 (2004).
[4] Y. Luo, W. W. Heidbrink, K. H. Burrell, D. H. Kaplan, and P. Gohil, Rev. Sci. Instrum. **78**, 033505 (2007).
[5] M. Osakabe, S. Yamamoto, K. Toi, Y. Takeiri, S. Sakakibara, K. Nagaoka, K. Tanaka, K. Narihara, and the LHD Experimental Group, Nucl. Fusion **46**, S911 (2006).
[6] S. Murakami, H. Yamada, M. Sasao, M. Isobe, T. Ozaki, T. Saida, P. Goncharov, J. F. Lyon, M. Osakabe, T Seki, Y. Takeiri, Y. Oka, K. Tumori, K. Ikeda, T. Mutoh, R. Kumaawa, K. Saito, Y. Torii, T. Watari, A. Wakasa, K. Y. Watanabe, H. Funaba, M. Yokoyama, H. Maassberg, C. D. Beidler, A. Fukuyama, K. Itoh, K. Ohkubo, O. Keneko, A. Komori, O. Motojima, and LHD Experimental Group, Fusion Sci. Technol. **46**, 241 (2004).
[7] D. Reiter, M. Baelmans, and P. Börner, Fusion Sci. Technol. **47**, 172 (2005).

Downloaded 19 Jun 2011 to 130.54.110.71. Redistribution subject to AIP license or copyright; see http://rsi.aip.org/about/rights_and_permissions